Electrochimica Acta, Vol. 35, No. 9, pp. 1337–1343, 1990
Printed in Great Britain.

0013–4686/90 $3.00 + 0.00

ELECTROCHEMICAL BEHAVIOUR OF COPPER IN AQUEOUS MODERATE ALKALINE MEDIA, CONTAINING SODIUM CARBONATE AND BICARBONATE, AND SODIUM PERCHLORATE

M. PÉREZ SÁNCHEZ,* M. BARRERA,* S. GONZÁLEZ* and R. M. SOUTO†
*Dpto Química Física and †Dpto Física Fundamental y Experimental, Universidad de La Laguna, Tenerife, España

R. C. SALVAREZZA and A. J. ARVIA
INIFTA, Universidad Nacional de La Plata, Argentina

(*Received* 19 *September* 1989; *in revised form* 16 *November* 1989)

Abstract—The voltammetric polarization of Cu specimens in Na_2CO_3, $NaHCO_3$ and $NaClO_4$ solutions (8–12 pH range) has been investigated. Voltammetry data were complemented with SEM and electron microprobe analysis. Results are found to be in agreement with the passivation model developed for Cu in plain NaOH solutions. For the latter the process can be described in terms of two steps, namely, at low potentials the initial formation of a Cu_2O thin layer followed by the growth of a massive Cu_2O layer, and at higher potentials the appearance of a CuO–$Cu(OH)_2$ layer. These processes are accompanied by the formation of soluble Cu species. Beyond a certain potential which increases with the solution pH, copper pitting takes place. This model can be extended to Cu in carbonate/bicarbonate containing solutions by considering that Cu carbonates precipitate as long as soluble ionic Cu species are produced, without interfering appreciably with the formation of Cu oxides. The appearance of copper carbonate species is enhanced when pitting corrosion sets in. The precipitation of Cu carbonates occurs principally around pits. Cu pitting, although it is observed for all solutions, becomes more noticeable at the lowest pH values. At a constant pH, the density of pits increases in the order $NaClO_4 > NaHCO_3 > Na_2CO_3$. The influence of the electrolyte composition on Cu pitting is closely related to the blockage capability for pit nucleation and growth of the corresponding copper salts. Passivation in the Cu_2O–$Cu(OH)_2$ region hinders pitting corrosion.

Key words: copper, pitting corrosion, passivation, alkaline media.

1. INTRODUCTION

The corrosion, passivation and pitting corrosion of copper have been studied in different solutions since more than three decades ago. The literature on the subject until 1980 is reviewed in references[1, 2]. The potential–pH diagrams of the Cu–H_2O system have been calculated for several binary and multicomponent systems at 25°C[2, 3]. For the binary Cu–H_2O and for the ternary Cu–CO_2–H_2O systems, these diagrams indicate that the stable forms of copper at pH 8 and 11 are Cu_2O and CuO, whereas in the presence of HCO_3^- at pH 8 the species $CuCO_3$–$Cu(OH)_2$ (malachite) should also be included. Likewise, in this case a decrease in pH makes the formation of $2CuCO_3$–$Cu(OH)_2$ (azurite) possible. Similarly, in Na_2CO_3-containing solutions at pH 11, the stable forms are Cu_2O, CuO and complex anionic species containing copper. This is summarized in Table 1.

Recently, the composite nature of the passive layer formed on copper in basic solutions was established. In this case there is a general agreement that the passive layer is made up of an inner Cu_2O layer, followed by a CuO layer, and finally an outer $Cu(OH)_2$ layer[4]. The entire layer structure undergoes short and long time range phase transitions[5–11]. It has also been demonstrated that the passive layer formation also involves the appearance of Cu(I) and Cu(II) soluble species[10, 12, 13]. Beyond a certain threshold potential, which depends considerably on the solution composition, the breakdown of the passive layer and the initiation of copper pitting can be observed[2, 12].

Despite the number of publications about copper corrosion and passivity, the kinetics of the various complex processes involved in them has been investigated less extensively than for other metals. Therefore, it is interesting both from the fundamental and practical standpoint to study the influence of HCO_3^- and CO_3^{2-} ions on those processes. These ions, which are usually found in natural waters, may assist either the corrosion or the protection of copper depending on the ambient conditions, particularly the operating range of pH.

This report refers to a comparative corrosion study of copper in moderate alkaline solutions containing different $NaHCO_3/Na_2CO_3$ concentration ratios, and in $NaClO_4$ solutions at various pH, by using conventional voltammetry complemented with SEM

Table 1. Thermodynamic data of copper in Na_2CO_3 + $NaHCO_3$ solutions at 25°C taken from refs [2, 3, 13]

(a) Electrode oxidation reactions	Electrode potential/V *vs sce*
$2Cu + H_2O = Cu_2O + 2H^+ + 2e^-$	$E_0 = 0.229 - 0.0591$ pH
$Cu + H_2O = CuO + 2H^+ + 2e^-$	$E_0 = 0.328 - 0.0591$ pH
$Cu + 2H_2O = CuO \cdot H_2O + 2H^+ + 2e^-$	$E_0 = 0.367 - 0.0591$ pH
$Cu_2O + H_2O = 2CuO + 2H^+ + 2e^-$	$E_0 = 0.427 - 0.0591$ pH
$Cu_2O + 2H_2O = 2CuO \cdot H_2O + 2H^+ + 2e^-$	$E_0 = 0.505 - 0.0591$ pH

(b) Ionic equilibria	log K (ionic strength = 0)
$CO_3^{2-} + 2H^+ = HCO_3^-$	10.33
$HCO_3^- + H^+ = H_2CO_3$	6.35
$Cu^{2+} + CO_3^{2-} = CuCO_3$	6.75
$Cu^{2+} + 2CO_3^{2-} = [Cu(CO_3)_2]^{2-}$	9.92
$CuCO_3(s) = Cu^{2+} + CO_3^{2-}$	−9.63
$Cu(OH)_2(CO_3)Na_2(s) = Cu^{2+} + 2OH^- + CO_3^{2-} + 2Na^+$	−15.0
$CuCO_3 \cdot Cu(OH)_2$(s, malachite) $= 2Cu^{2+} + 2OH^- + CO_3^{2-}$	−33.78
$2CuCO_3 \cdot Cu(OH)_2$(s, azurite) $= 3Cu^{2+} + 2OH^- + 2CO_3^{2-}$	−45.96

(c) pH range	Cu-containing species (0.1 M CO_2 solution)
$3 \leq$ pH ≤ 5.5	Cu^{2+}; CuO; $CuCO_3$; $Cu(OH)_2$; $2CuCO_3 \cdot Cu(OH)_2$; H_2CO_3
$5.5 \leq$ pH ≤ 10.3	$CuCO_3$(aq); $Cu(CO_3)_2^{2-}$; $CuCO_3 \cdot Cu(OH)_2$; HCO_3^-
$10.3 \leq$ pH ≤ 14	CuO; CuO_2^{2-}; $CuCO_3 \cdot Cu(OH)_2$; $2CuCO_3 \cdot Cu(OH)_2$; $HCuO_2^-$; $CuCO_3(OH)_2^{2-}$; CO_3^{2-}

observations and electron microprobe analysis. The properties of the passivating layers produced on copper depend on the solution composition as well as the conditions for the initiation of pitting corrosion.

2. EXPERIMENTAL

Solutions were prepared from twice-distilled water and analytical grade chemicals. The following solution compositions were employed x M Na_2CO_3 + $(0.1-x)$ M $NaHCO_3$ in the 8.5–11.5 pH range and 0.1 M $NaClO_4$ solutions in the 9–11.5 pH range, the solution pH being adjusted by adding controlled amounts of diluted NaOH solution.

Measurements were performed in a three-electrode electrochemical cell. Working electrodes consisted of flat discs (0.3 cm dia.) resulting from transverse cuttings of electrolytic Cu rods (99.9% purity) as received without any further thermal treatment. Each working electrode was mounted at a rotating disc electrode device to be used under either still or rotation conditions in the 0–1200 rpm range. The electrode surface was mirror-polished by employing a gradual sequence of fine grained emery papers ranging from 30 to 5 μm grit. Each polished specimen was successively rinsed in a.r. grade acetone, twice distilled water and finally, dried in air at room temperature. The contact between the working electrode surface and the solution was made through the hanging electrolyte meniscus technique proposed for a single crystal electrode mounting[14]. In this case, the insulating shroud that is usually employed in conventional rotating disc electrode devices to preserve the semi-infinite hydrodynamic boundary conditions does not appear to be essential[15]. The absence of side effects has been concluded from the behaviour of several adsorption systems.

The potential of the working electrode was measured against a sodium chloride saturated calomel electrode (*sce*). The counter electrode was a cylindrical platinum mesh surrounding the working electrode. Runs were made at 25.0 ± 0.1°C under an Ar atmosphere.

A new fresh mirror-polished disc electrode was used for each run. The experiment was started by potential cycling the working electrode at 0.01 V s^{-1} between about −0.65 and 0.0 V for $NaClO_4$ solutions, and from −0.80 to 0.6 V thereabouts, for $NaHCO_3$ + Na_2CO_3 solutions so that the mechanical stress produced by the polishing technique at the electrode surface was relieved[16]. This treatment allowed us to establish through the voltammograms stable and reproducible starting conditions for the experiments.

Single (STPS) and repetitive triangular potential sweeps (RTPS) were applied to the working electrode at scan rate 0.01 V s^{-1}. SEM micrographs of the layer anodically formed were obtained with a Hitachi S-450 scanning electron microscope (SEM) at beam energies in the 20–25 kV range. SEM micrographs were complemented with electron microprobe analysis data.

3. RESULTS AND INTERPRETATION

3.1. *Voltammetric data*

Voltammograms run with 0.2 M $NaClO_4$ at pH 9.1 (Fig. 1a) exhibit in the positive potential going scan a well defined peak at −0.24 V (peak Ia) which is related to the Cu_2O electroformation. At potentials more positive than 0.02 V a remarkable current in-

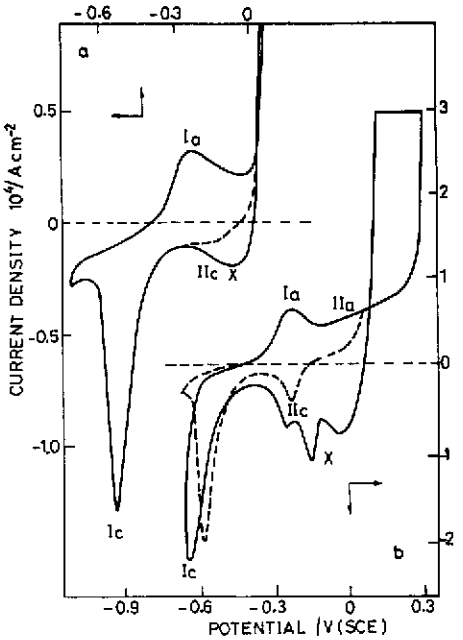

Fig. 1. Stabilized voltammograms of copper in 0.1 M $NaClO_4$ at 0.01 V s^{-1}: (a) pH 9.1; (b) pH 11.0; 25°C.

crease is detected. The negative scan shows a considerable hysteresis in the anodic current preceding a broad cathodic peak, X, at 0.0 V which partially masks other cathodic contributions. Thus, when the potential is reversed at values slightly more negative than 0.02 V (Fig. 1a, dashed line), the small cathodic current peak IIc can be detected at −0.15 V and, simultaneously, peak X disappears. SEM observations of the electrode surface reveal that the large anodic current and the corresponding hysteresis is due to the nucleation and growth of pits on the Cu surface, whereas peak X is related to the electroreduction of soluble Cu(II)-species produced during the electrodissolution. Peaks IIc and Ic can be attributed to the electroreduction of CuO–$Cu(OH)_2$ to Cu_2O and to the electroreduction of Cu_2O to Cu, respectively.

The voltammograms run in 0.2 M $NaClO_4$ at pH 11 (Fig. 1b) show, in principle, the same features as those already described at the lower pH. It should be noted, however, that Cu pitting occurs now at potentials more positive than 0.2 V. Accordingly, the broad peak IIa related to the CuO–$Cu(OH)_2$ electroformation can be observed and the passive region becomes broader. Likewise, by setting the potential within the pitting potential region, the subsequent negative potential going scan comprises a relatively large electroreduction charge (peak X) which can also be attributed to the electroreduction of soluble species. The potentials of peaks I and II shift to more negative values with increasing pH in agreement with the thermodynamic predictions of the different Cu(0)/Cu/(I) and Cu(0)/Cu(II) electrode reactions as seen in Table 1[2, 3] (Figs 1a and b). It should also be noted that the protective characteristics of the passive layer at pH 11 are better than at lower pH. Furthermore, the reverse scan also shows a considerable hysteresis of the anodic current related to Cu electrodissolution. The voltammograms run with 0.09 M $NaHCO_3$ + 0.01 M Na_2CO_3 (pH 9.1) exhibit two anodic current peaks which are progressively discovered as the anodic switching potential is set more positive than 0.0 V (Fig. 2a). These peaks, Ia at −0.24 V and IIa at −0.05 V, are comparable to those assigned to the formation of Cu_2O and CuO, respectively, in both plain NaOH solutions[9] and 0.1 M $NaClO_4$ as referred to above. As the anodic switching potential is above 0.0 V, a rather extended passive region in the voltammogram (IIIa) can be distinguished. At potentials more positive than 0.4 V, the voltammogram shows a number of periodic current oscillations which are typical of rupture and reforming events occurring at the passive layer. These events are associated with the initiation of pitting corrosion. However, it is evident that in the $NaHCO_3$ + Na_2CO_3-containing solution pitting becomes a more rare event. Passivation in the potential range of the Cu_2O–CuO–$Cu(OH)_2$ tends to hinder pit nucleation at least for short time range polarization at 0.3 V. Therefore, the absence of hysteresis in the anodic current indicates that after nucleation pit growth is hindered, probably by the precipitation of insoluble salts into the pit. On the other hand, when the anodic switching potential definitely enters the passivation region a new cathodic peak IIIc shows

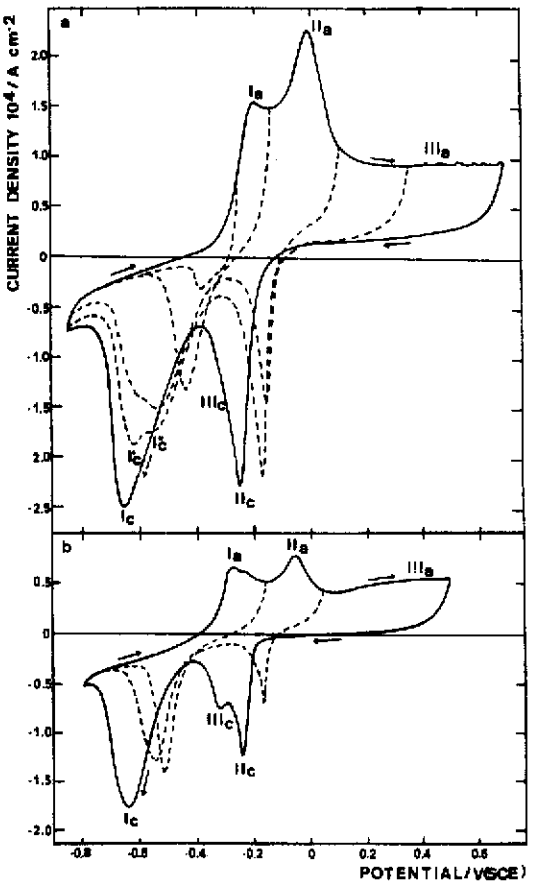

Fig. 2. Stabilized voltammograms of copper in $NaHCO_3$ + Na_2CO_3 solutions at 0.01 V s^{-1}: (a) 0.09 M $NaHCO_3$ + 0.01 M Na_2CO_3, pH 9.1; (b) 0.03 M $NaHCO_3$ + 0.07 M Na_2CO_3, pH 11.

up at −0.25 V during the negative potential going excursion. This new peak only appears in the $NaHCO_3 + Na_2CO_3$ solutions. In addition the shape and position of peak IIc strongly depends on the value of the anodic switching potential, as has already been observed for Cu in NaOH solutions[10].

The voltammogram run in 0.03 M $NaHCO_3$ + 0.07 M Na_2CO_3 (pH 11) indicates a remarkable contribution of Cu_2O massive formation (peak Ia) and the subsequent electroformation of CuO–$Cu(OH)_2$ at −0.1 V (peak IIa) (Fig. 2b). In this case, the relative contribution of peak IIa becomes greater than that observed for 0.1 M $NaClO_4$. The appearance of only two peaks, IIc and Ic, on the reverse potential scan can be observed when the anodic switching potential is kept below 0.01 V, *ie* in the region at which CuO–$Cu(OH)_2$ is formed. However, when the anodic switching potential is set above 0.01 V, peak IIc becomes considerably distorted due to the presence of peak IIIc. Likewise, the height of peak IIIc decreases as the amount of soluble ionic Cu species diminishes, a fact which can be followed through the shift of the baseline in the voltammogram.

Similar voltammetric behaviour is observed for 0.1 M $NaHCO_3$ and 0.1 M Na_2CO_3 (pH 8.7 and 11.3), although in both solutions peak IIIc begins to appear when the anodic switching potential is more positive than 0.0 V. Therefore, the comparison of the voltammograms in the different Na_2CO_3–$NaHCO_3$ containing solutions provides a clear idea about the influence of Na_2CO_3 and $NaHCO_3$ concentration and pH on various aspects of entire processes, namely, the corrosion and passivation of Cu in moderate alkaline solutions, the initiation of pitting and the electroreduction behaviour of the passivating layer, but further details come out from the influence of stirring produced by using the Cu *rde* (Fig. 3).

The influence of stirring is more clearly noticed at pH 8.7, and it can be summarized as follows:

(i) The anodic to cathodic voltammetric charge ratio increases according to the rate of stirring. Likewise, the distribution of the anodic peaks changes, for instance, the relative contribution of peak Ia diminishes as compared to the current recorded at more positive potential.

The voltammetric profile under stirring and at high positive potentials presents a large number of oscillations which are directly related to an enhancement of pitting corrosion.

(ii) Stirring also modifies the electroreduction voltammogram, particularly in decreasing the height of peaks IIc and IIIc. Furthermore, the shape of peak Ic is also considerably changed.

(iii) The repetitive voltammograms show a progressive although rather slow increase of the entire voltammetric charge. This effect can be interpreted through an increase of the active area of the Cu specimen produced by the electrodissolution process.

The *rde* data confirm that the amount of soluble ionic Cu species is enhanced by stirring, presumably through the removal of Cu carbonate constituents precipitated at the anodic layer level. It should be noted that peak IIIc, which appears in the $Na_2CO_3 + NaHCO_3$ solutions, can be assigned to a soluble copper carbonate containing Cu ionic species originated at the reaction interface (see Table 1c).

3.2. *SEM micrographs*

The appearance of pits at the Cu surface after the potential cycling of the specimen in the different solutions was followed through SEM micrographs (Fig. 4).

At pH values ranging between 8.5 and 9 the largest pitting corrosion effect is found for 0.1 M $NaClO_4$ (Fig. 4a). In this case, nearly spherical pits, most of them around a common average diameter of about 3.50–4.00 μm are formed. During the growth process a number of those pits overlapped. In the same solution at pH 11 (Fig. 4b) a milder pitting corrosion and a much lower pit density is observed. Otherwise, in $NaHCO_3 + Na_2CO_3$ solutions at pH 8.8 (Fig. 4c) a clear pitting corrosion can also be seen although less intense than in 0.1 M $NaClO_4$ at the same pH. An enlarged pit image resulting for a Cu specimen in $NaHCO_3 + Na_2CO_3$ solution at pH 9.5 after a prolonged holding at potentials greater than 0.4 V (Fig. 4d) reveals that each pit is surrounded by an outer salt formation which displays a sort of outer volcano-shaped structure. The SEM micrographs obtained in the $NaHCO_3 + Na_2CO_3$ solutions at a higher pH tend to show a rather more homogeneous attack and to some extent a milder localized corrosion. In this case the prolonged anodization at high positive potentials produces a relatively much smaller density of pits.

3.3. *Electron microprobe analysis data*

The presence of Cu carbonate species at the passive layer was determined by electron microprobe analysis on Cu electrode surfaces which have been anodized in $NaHCO_3 + Na_2CO_3$ solutions. The corresponding carbon signal can already be observed at anodization potentials located in the potential range of peak Ia, *ie* in the potential range of Cu_2O formation. In this case, after 20 min anodization the intensity of the C signal is twice that of the blank, and it continues to increase as the potential is gradually shifted positively. By holding the specimen at a potential set within the passivation region, the anodic surface layer exhibits a considerable increase of the C signal. In this case, the number of counts reaches a value six times greater than that found for the blank.

4. DISCUSSION AND CONCLUSIONS

The electrochemical behaviour of Cu in alkaline solutions is rather complex as it comprises several reactions, namely the electroformation and electroreduction of different Cu oxide and hydroxide layers and the simultaneous formation of Cu(I) and Cu(II) soluble species.

The relative contribution of all these reactions depends on the potential and time windows used in the experiments as well as on the solution stirring. As demonstrated earlier[10, 12] the potential range of the different processes can be estimated from the thermodynamic data assembled in Table 1.

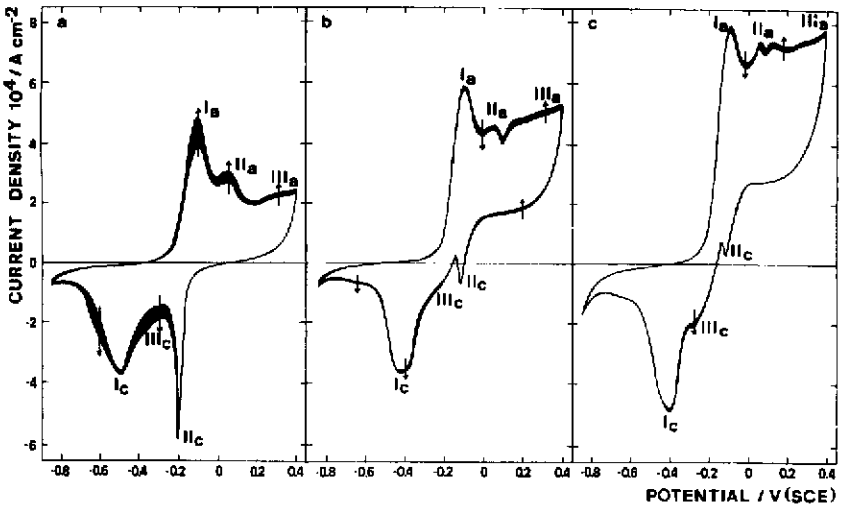

Fig. 3. Repetitive voltammograms of copper in 0.1 M $NaHCO_3$ at different rotation speed of the working electrode (at 25°C): (a) 0; (b) 540; (c) 1140 rpm. The arrows indicate the variation of the voltammogram along the potential cycling.

The experimental results show that the passivation of Cu in the different solutions employed in this work initiates at relatively low potentials through the formation of a Cu_2O layer, probably through a two step process, namely, the formation of a very thin layer Cu(OH) followed by the formation of a massive Cu_2O layer (peak Ia)[10, 12]. At higher potentials the second oxidation level is reached, *ie* the CuO–$Cu(OH)_2$ layer is produced, so that a composite anodic layer is formed[4, 10, 11]. At potentials about 0.0 V soluble ionic Cu species are also produced. The electroreduction of the latter contributes to the considerable increase in the cathodic current observed along the voltammograms particularly at the lowest pH and in 0.1 M $NaClO_4$ solutions.

It is clear that the same reactions occur, at least qualitatively, in the presence of $NaHCO_3$ and Na_2CO_3 solutions. Nevertheless, in this case the concentration of soluble ionic Cu species depends on the solubility product of basic Cu carbonates ($CuCO_3$–$Cu(OH)_2$ or $2CuCO_3$–$Cu(OH)_2$) (Table 1b) which precipitate at the outer passive layer region as seen in the SEM micrographs (Fig. 4). In principle, the formation of Cu carbonates does not interfere with the first and second levels of the Cu electrooxidation processes. In this case, the formation of Cu oxides is thermodynamically and kinetically favoured as compared to the formation of precipitated $CuCO_3$.

At the initiation of the anodic reaction the Cu–OH^- ion interaction should be stronger than the Cu–CO_3^{2-} ion or Cu–HCO_3^- ion interactions as one can conclude from the corresponding polarizabilities of the ions[17]. Accordingly, the electroreduction of the composite passive layer should start at the level of the CuO layer, and subsequently be followed by the electroreduction of carbonate-containing Cu constituents of the anodic layer. The contribution of the latter process, which is related to peak IIIc, depends on the amount of carbonate, although peak IIIc can partially overlap both peaks IIc and Ic.

At the passive region, pitting corrosion is preceded by the typical current fluctuations associated with the local breakdown and reforming of the passive layer. According to data in the literature[2], the pitting potential of Cu in CO_2-containing aqueous media at pH 3.5 is *ca* −0.13 V. On the basis that the pitting potential values shift positively 0.06 V/pH unit at 25°C[18], the values of the pitting potential of Cu are 0.40 V at pH 8.7 and 0.53 V at pH 11. The first value closely coincides with the potential at which the current fluctuations begin to appear in region IIIa (Fig. 2a). This fact is observed for all solutions although as should be expected it is more remarkable at the lowest pH values. Conversely, as the anodic switching potential is slightly more negative than the corresponding pitting potential (Fig. 2b), no clear Cu pitting is established, but mainly a nearly homogeneous Cu electrodissolution through the anodic layer. These results can be satisfactorily correlated to SEM micrographs for the Cu specimen treated in the $NaHCO_3 + Na_2CO_3$ solutions (Fig. 4). At a constant pH pitting appears to be greater in $NaClO_4$ than in $NaHCO_3 + Na_2CO_3$ solutions as for the former case; the corresponding Cu salts, being much more soluble than for the latter, should exhibit a much poorer capability for inhibiting Cu pit growth. Nevertheless, it should be noted that for the $Na_2CO_3 + NaHCO_3$ solutions the local acidification related to the build-up of passivity, according to the reactions shown in Table 1, implies a local increase in the concentration of HCO_3^- ion in such a way that the latter should be considered as the actual aggressive ion for Cu pitting. This fact explains the pH dependence of the pitting potential. Moreover, as soluble ionic Cu species are involved in phase equilibria with insoluble Cu carbonate species, one should expect, therefore, that the latter appear concentrically distributed around the pits, as seen through SEM micrographs. These conclusions agree with those obtained for other metals such as Fe and Ni, in $NaHCO_3 + Na_2CO_3$ solutions, in which the HCO_3^- ion appears to be mainly responsible for the localized corrosion[19, 20].

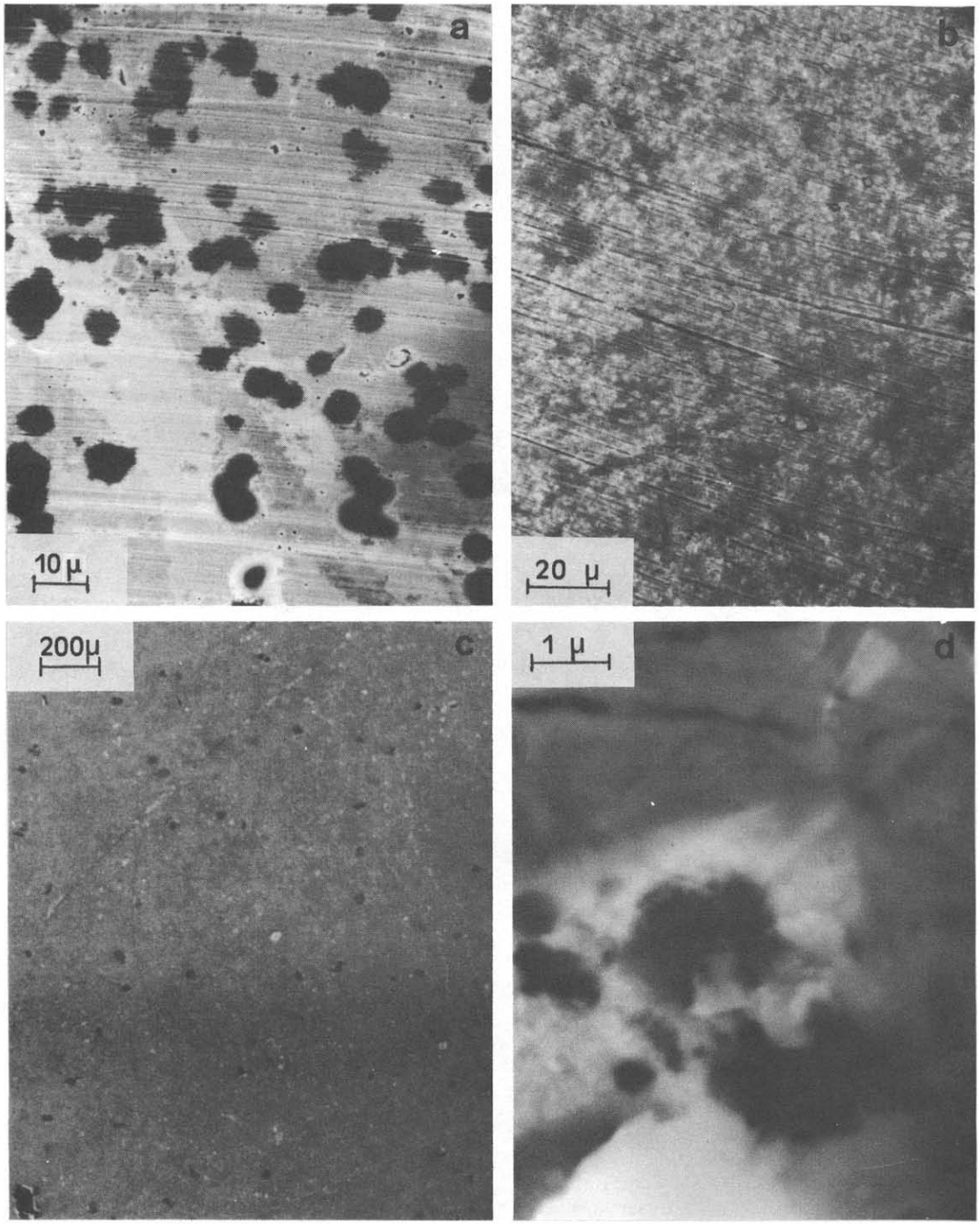

Fig. 4. SEM micrographs of copper electrodes after treatment in different solutions (at 25°C): (a) 0.1 M $NaClO_4$, pH 9.1; (b) 0.1 M $NaClO_4$, pH 11.0; (c) 0.09 M $NaHCO_3$ + 0.01 M Na_2CO_3, pH 9.1; (d) 0.03 M $NaHCO_3$ + 0.07 M Na_2CO_3, pH 11.

Acknowledgements—Financial support for this work by the Gobierno de Canarias (Dirección General de Universidades e Investigación) under Contract No. 46/01.06.88, is gratefully acknowledged. A.J.A. thanks the Faculty of the Universidad de La Laguna for the invitation to cooperate with the Departamento de Química-Física during June–July 1988. A fellowship from the Consejo Nacional de Investigaciones Científicas y Ténicas (Argentina) to R.C.S. is gratefully acknowledged.

REFERENCES

1. U. Bertocci and D. Turner, in *Encyclopedia of Electrochemistry of the Elements* (Edited by A. J. Bard), Vol. II, Marcel Dekker, New York (1974).
2. J. Van Muylder, in *Comprehensive Treatise of Electrochemistry* (Edited by J. O'M. Bockris, B. E. Conway, E. Yeager and R. E. White), Vol. 4, pp. 1–96, Plenum Press, New York (1981).

3. M. Pourbaix, in *Atlas of Electrochemical Equilibria in Aqueous Solutions*, pp. 384–392, Pergamon Press, London (1965).
4. H. D. Speckmann, M. M. Lohrengel, J. W. Schultze and H. H. Strehblow, *Ber. Bunsenges. Phys. Chem.* **89,** 392 (1985).
5. D. W. Shoesmith, T. E. Rummery, D. Owen and W. Lee, *J. electrochem. Soc.* **123,** 790 (1976).
6. V. Ashworth and D. Fairhust, *J. electrochem. Soc* **123,** 506 (1977).
7. M. R. G. Chialvo, S. L. Marchiano and A. J. Arvia, *J. appl. Electrochem.* **14,** 165 (1984).
8. H. H. Strehblow and H. D. Speckmann, *Werkstoffe Korros.* **35,** 512 (1984).
9. M. R. G. Chialvo, J. O. Zerbino, S. L. Marchiano and A. J. Arvia, *J. appl. Electrochem.* **16,** 517 (1986).
10. J. Gómez Becerra, R. C. Salvarezza and A. J. Arvia, *Electrochim. Acta* **33,** 613 (1981).
11. M. Wagner, H. Wiese and K. G. Weil, *Ber. Bunsenges. Phys. Chem.* **92,** 736 (1988).
12. M. R. G. Chialvo, R. C. Salvarezza, D. Vásquez Moll and A. J. Arvia, *Electrochim. Acta* **30,** 1501 (1985).
13. R. M. Smith and A. E. Martell, *Critical Stability Constants*, Vol. 4, Pergamon Press, New York (1976).
14. D. Dickertmann, F. D. Koppitz and J. W. Schultze, *Electrochim. Acta* **21,** 967 (1967).
15. B. D. Cahan and H. M. Villullas, Proc. VIII Reunión Latinoamericana de Electroquímica y Corrosión, paper 1.60, p. 234, Huerta Grande, Córdoba, Argentina (1988).
16. U. Bertocci and D. R. Turner, in *Encyclopedia of the Electrochemistry of the Elements* (Edited by A. J. Bard), Vol. II, p. 385, Marcel Dekker, New York (1974).
17. J. M. West, *Electrodeposition and Corrosion Processes*, Van Nostrand, London (1965).
18. J. M. Galvele, *J. electrochem. Soc.* **124,** 464 (1976).
19. E. B. Castro, C. R. Valentini, C. A. Moina, J. R. Vilche and A. J. Arvia, *Corros. Sci.* **26,** 781 (1986).
20. A. E. Bohé, J. R. Vilche and A. J. Arvia, *J. appl. Electrochem.* **14,** 645 (1984).